

An Effort on Homogenizing Size Distribution of Magnetic Nanosphere Fe_3O_4 -Poly-Lactic Acid for Hyperthermia Treatment

Grace Tj. Sulungbudi and Mujamilah

Center for Science and Technology of Advanced Materials, BATAN

Kawasan Puspiptek, Serpong, Tangerang, 15314, Indonesia

Email: ian@batan.go.id

Diterima: 01-Feb-2016 Diperbaiki: 18-Mar-2016 Disetujui: 24-Mei-2016

ABSTRACT

An Effort on Homogenizing Size Distribution of Magnetic Nanosphere Fe_3O_4 -Poly-Lactic Acid for Hyperthermia Treatment. An effort on homogenizing the size distribution of magnetic nanosphere (MN) base on Fe_3O_4 nanoparticle coated by Poly-lactic acids (PLA) has been carried out. MN synthesis parameters were optimized to obtain MN with narrow size distribution, but still maintaining other properties especially its magnetic property. The synthesis process was then followed by sequential centrifugation with different speed for selective separation of MN with different size distribution. The size distribution characteristics of the MN were evaluated by Scanning Electron Microscope (SEM), Transmission Electron Microscope (TEM), and Particle Size Analyzer (PSA). As a result, fractional MNs having different size distribution smaller than 400 nm were successfully obtained. The highest fraction was achieved for MN with size distribution < 150 nm, which was almost reaching 73% of total weight. However, the colloidal stability was still rather poor due to agglomeration tendency of MN which was observed clearly in its SEM and TEM images. The magnetic properties were analyzed by Vibrating Sample Magnetometer (VSM), which gave the saturation magnetization (M_s values). These values were slightly affected by the MN size distributions with maximum M_s value of 15.3 emu/g. Considering the composition used within the experiment and from the M_s values, the Fe_3O_4 nanoparticle loading efficiency of around 78.9% could be determined. Referring to these results, the colloidal stability problem could be overcome by co-polymer grafting on PLA surface, hence the MN could be expected to be applied for magnetic hyperthermia based therapy.

Keywords: magnetic nanosphere, Fe_3O_4 , poly-lactic acids, size distribution, magnetic hyperthermia

ABSTRAK

Upaya Homogenisasi Distribusi Ukuran Nanosfer Magneti (MN) Fe_3O_4 -Poli Asam Laktat untuk Terapi Hipertermia. Upaya untuk menghomogenkan

distribusi ukuran nanosfer magnetik (MN) nanopartikel Fe₃O₄ yang dilapisi oleh poli asam laktat (PLA) telah dilakukan. Parameter sintesis MN dioptimalkan untuk mendapatkan MN dengan distribusi ukuran sempit, namun tetap menjaga sifat lainnya terutama sifat magnetiknya. Proses sintesis kemudian diikuti dengan sentrifugasi sekuensial dengan kecepatan yang berbeda untuk pemisahan selektif MN dengan distribusi ukuran yang berbeda. Karakteristik distribusi ukuran MN dievaluasi dengan Scanning Electron Microscope (SEM), Transmission Electron Microscope (TEM), dan Particle Size Analyzer (PSA). Hasilnya menunjukkan fraksional MN yang memiliki distribusi ukuran lebih kecil dari 400 nm berhasil diperoleh. Fraksi tertinggi dicapai untuk MN dengan distribusi ukuran <150 nm, yang hampir mencapai 73% dari berat total. Meskipun demikian, stabilitas koloid masih agak buruk karena MN cenderung mengalami aglomerasi yang teramati secara jelas pada gambar SEM dan TEM-nya. Sifat magnetik dianalisis dengan Vibrating Sample Magnetometer (VSM), yang memberikan magnetisasi saturasi (nilai Ms). Nilai ini sedikit dipengaruhi oleh distribusi ukuran MN dengan nilai Ms maksimum 15,3 emu/g. Dengan mempertimbangkan komposisi yang digunakan dalam percobaan dan dari nilai Ms, efisiensi kadar nanopartikel Fe₃O₄ sekitar 78,9% dapat ditentukan. Mengacu pada hasil ini, masalah stabilitas koloid dapat diatasi dengan pencangkakan ko-polimer pada permukaan PLA, sehingga MN diharapkan dapat diterapkan untuk terapi hipertermia.

Kata Kunci: *nanosfer magnetik, Fe₃O₄, poli asam laktat, distribusi ukuran, hipertermia magnetik*

INTRODUCTION

Hyperthermia (also called thermal therapy or thermotherapy) is a type of cancer treatment in which body tissue is exposed to high temperatures (up to 113°F) which can damage and kill cancer cells, usually with minimal injury to normal tissues. Currently, three different particles heating technologies for therapeutic purposes are being explored: optical heating using lasers [1]; ultrasound heating of small bubbles [2]; and magnetic nanoparticle (MNP) heating due to alternating magnetic field [3]. Optical methods heat particles effectively, but are severely limited by the attenuation of the laser light by tissue. Ultrasound heating may ultimately be promising, as the energy is focused to a selected location. This technique, however, suffers from speed of sound variation in most tissues. MNP heating can be accomplished at depths necessary for treatment of tumors located virtually anywhere in the human body. The same MNP used for heating may also be sufficient for medical imaging uses. Referring to these reasons, MNP based hyperthermia are more promising and intensively being studied nowadays [3].

For such biomedical applications, MNPs should have good colloidal and physico-chemical stability. There are several strategies of surface functionalization using different coating agents and biomolecules that are beneficial to achieve such stable colloid magnetic sample. A suitable particle surface modification or coating is also a useful tool to improve their biocompatibility and decrease as much as possible their toxicity. These surface modification plays a crucial role in improving MNPs specificity, hence the higher the targeting specificity, the more selective of target cancer cells will be achieved [4].

One of particle systems widely developed for this application is magnetic nanosphere (MN) consists of MNP of Fe_3O_4 coated by polymer such as poly-lactic acids (PLA). PLA is a type of polymer with potential applications in nanomedicine as carriers of drugs, proteins and genes that offers several benefits, such as biocompatibility, biodegradability and sustainable therapeutic drug release over prolonged periods, due to their polymer matrix allowing the control of drug release kinetics [5]. Previous studies have evaluated the cytotoxic potential of PLA in different cell types and concluded that PLA-nanoparticles were non-cytotoxic [6]. Meanwhile Fe_3O_4 is one of MNP type that is intensively developed recently for biomedical application due to its biocompatibility and its high magnetic properties [7]. This high magnetic property is an important factor in biomedical applications such as for generating heat in hyperthermia based therapy and developing image contrast in magnetic resonance imaging (MRI) based diagnostic procedure. The biocompatibility of Fe_3O_4 -PLA microsphere was evaluated by a series of in vivo and in vitro tests, and showed that magnetic microsphere inhibited liver cancer cell proliferation, lacked hemolysis activity, and no genotoxic effects. Therefore, applying PLA/ Fe_3O_4 microsphere as drug carrier not only has good targeting capacity, but also helps to control cancer cell growth by toxicity effect of carrier and enhance targeted drug efficiency [8].

On the other side, thorough investigation showed that intrinsic features of nanoparticles, such as size, surface charge, agglomeration tendency, can also significantly affect the targeting capacity. An in vivo distribution study after intravenous injection of 10 to 250 nm size nanoparticles showed that nanoparticles smaller than 50 nm were found in almost all organs, including the blood, liver, spleen, kidneys, testes, thymus, heart, lungs and brain. Meanwhile, most nanoparticles larger than 50 nm were detected only in the blood, liver and spleen [9]. However, these nanoparticles feature will also affect MNPs magnetic properties especially its saturation magnetization, M_s value. For hyperthermia applications, it should be considered that MNPs must have as high M_s as possible, which will result in large thermal energy dissipation in the tumor cells [10].

In this study, we report an effort to optimize the synthesis process of Fe₃O₄-PLA nanosphere followed by a series of particle size selection process to obtain a homogeneous distribution of magnetic nanosphere. The morphology and magnetic characteristics of groups of MNs with narrower size distribution were analyzed to understand the potential application of this nanosphere in magnetic hyperthermia.

MATERIALS AND METHOD

Materials

The materials used in this study were Poly-lactic acid (PLA from Wako, Japan), Poly Vinyl Alcohol (PVA from Merck, Germany) 72000 Da, oil-based MNPs prepared according to Leamy et.al. [12], Chloroform from Merck and distilled water. The equipment used includes ultrasonic probe (SONIC ultrasonic processor models 750 VCX), Laboratory stirrer and JP SELECTA High Speed Refrigerated centrifuge models Medifriger-BL-S.

Preparation of MNP-PLA Nanosphere

Nanosphere preparation refers to a procedure conducted by previous researchers [13]. The process begins with the preparation of the primary solution of PLA 10% in chloroform and PVA 5% in distilled water. Nanosphere synthesis was carried out by the method of water-to-oil emulsion between the oil phase of the MNP-PLA and the aqueous phase of the PVA. The oil phase (phase 1) was prepared by mixing a solution of PLA and MNP with the mass ratio between MNP and PLA of 1.2/4.2, dispersed in chloroform. To obtain a homogeneous oil phase, the mixture was sonicated for 1 min, while the water phase (phase 2) was a solution of PVA in distilled water.

Emulsion process between the two phases was done by using sonication for 4 mins, referring to the methods of previous study [13]. After sonication the samples were then added to 500 mL of distilled water and stirred at 1000 rpm for 1 h, to evaporate the chloroform in water and allow for MNP coated with PLA to dry up in the water phase. After the chloroform evaporated, nanospheres were formed and dispersed in the water. The sample was then centrifuged at 9000 rpm for 15 mins and followed by triplicate washing step for removing PVA from nanosphere. For size selection process, the samples were recentrifuged with varying centrifugation speed of 1,000 rpm, 2,000 rpm, 5,000 rpm, 9,000 rpm and 12,000 rpm. The final samples obtained are codified as shown in Table 1. The synthesis was repeated twice to ensure the reproducibility of the process.

Nanosphere obtained were then characterized using PSA Malvern NanoZetasizer to obtain a dynamic size of nanosphere and its stability parameters in colloidal sample, SEM JEOL JSM-6390A and TEM JEOL JEM 1400 to understand the morphology and static size of nanosphere, and VSM OXFORD 1.2H to characterize the magnetic properties.

Table 1. Codification of nanosphere samples

No.	Sampel Code	Detailed Sample Information
1.	P1 and S1	Precipitate and Supernatant after centrifugation at 1,000 rpm
2.	P2 and S2	Precipitate and Supernatant after centrifugation at 2,000 rpm of S1 samples
3.	P5 and S5	Precipitate and Supernatant after centrifugation at 5,000 rpm of S2 samples
4.	P9 and S9	Precipitate and Supernatant after centrifugation at 9,000 rpm of S5 samples
5.	P12 and S12	Precipitate and Supernatant after centrifugation at 12,000 rpm of S9 samples

RESULT AND DISCUSSION

PSA Measurement

Figure 1 shows the size distribution curve of the nanosphere after sequential separation process as stated in Table 1. Figure 1 shows that particle size distribution peak tend to be more narrow for higher centrifugation speed. The average particle sizes of sample S1 are at 360 nm and 2,000 nm, S2 at 380 nm, S5 at 310 nm and S9 at 249 nm. The S12 sample could not be measured using PSA because the sample was very dilute. Another data measured using NanoZetasizer are some parameters related to colloidal stability as present at Table 2. The zeta potential measurement could not be carried out for S1 and S2 samples because the samples tend to agglomerate and causing sedimentation. The zeta potential values give the information of surface charge of nanosphere which will determine interaction behavior between nanosphere.

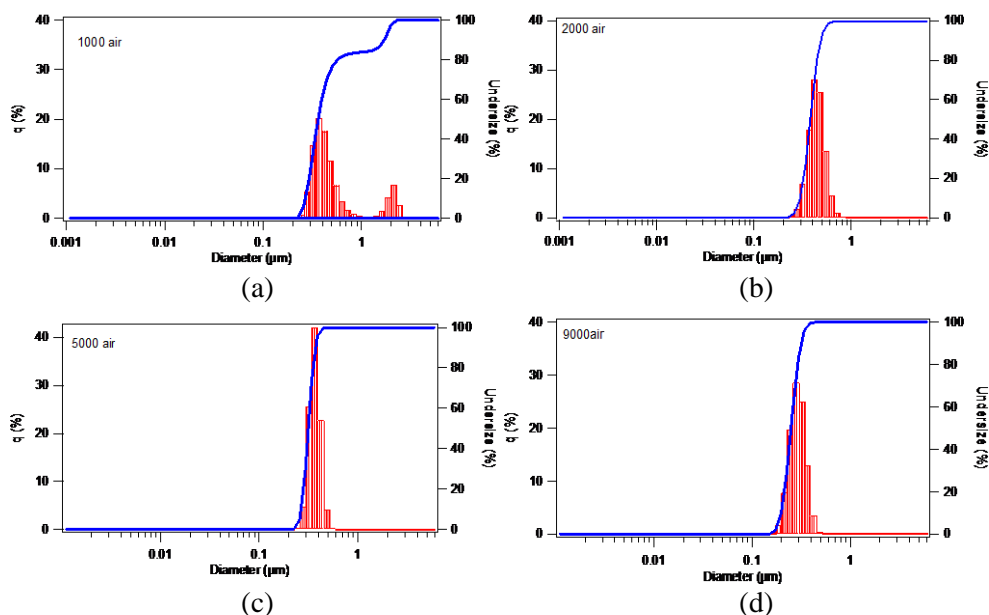


Figure 1. Size distribution curve of the nanospheres of samples: (a) S1, (b) S2, (c) S5, and (d) S9 measured using PSA technique

Table 2. Codification of nanosphere samples

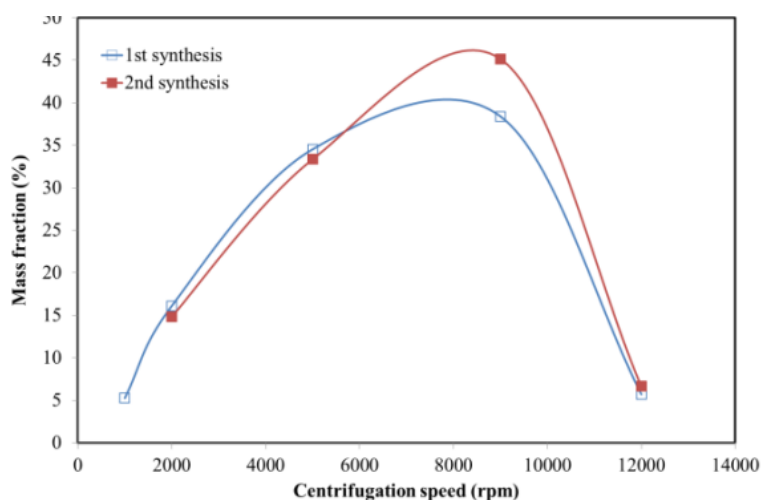
Sample	pH	Zeta Potential (mV)	Mobility (cm ² /Vs)	Conductivity (mS/cm)
S5	5	-6.10	-4.75 x 10 ⁻⁵	-0.0351
S9	5	-8.81	-6.873 x 10 ⁻⁵	-0.0102
S12	5	-9.14	-7.130 x 10 ⁻⁵	-0.0433

Mass Distribution

Mass distribution of the particles at each step of sequential centrifugation is presented in Table 3. The measurement was conducted in duplicate. The data presented graphically at Figure 2 shows that the largest distribution is achieved at 9,000 rpm centrifugation speed and obtained fairly good reproducibility. Compared to the initial stoichiometric calculation (total precursor of 1.68 g), the total yield reached 75.13% (1st-synthesis) and 65.30% (2nd-synthesis). These low total yields are caused by some of the material loss during the process and partly remains in the final supernatant (S12), which still shows a light brown color. Even on the first synthesis, precipitates can still be obtained after centrifugation at 12000 rpm speed, although the amount is very small. The second synthesis results showed a trend shift towards smaller grain size, but there is a decrease in total yield.

Table 3. Mass distribution of precipitate particles after sequential process of centrifugation

No.	Sample Code	Precipitate of nanoparticles			
		1 st -synthesis		2 nd -synthesis	
		Mass (mg)	%	Mass (mg)	%
1.	P1	66.40	5.258	-	-
2.	P2	203.32	16.099	162.87	14.835
3.	P5	436.16	34.536	366.16	33.350
4.	P9	485.04	38.406	495.77	45.157
5.	P12	72.00	5.701	73.09	6.658
Total yield (mg)		1,262.92		1,097.867	

**Figure 2.** Curve of mass distribution of precipitate particles after sequential process of centrifugation

SEM and TEM Observation

Overview of nanosphere morphology and size from SEM and TEM observations as a function of centrifugation speed are given in Figure 3 to Figure 5. SEM micrographs in Figure 3 generally show that the higher the centrifugation speed, a smaller size and more homogeneous nanosphere will be obtained. It appears that S1 samples have a size in the range of 100 nm to more than 1000 nm with a high tendency of agglomeration, while S2 samples have smaller and more homogeneous size in the range of 100 nm to nearly 1000 nm and lower agglomeration tendency. For S5 and S9 samples, homogeneous size with more separate nanosphere are clearly displayed and the average nanosphere size of 250 nm and 150 nm are measured for the two samples respectively.

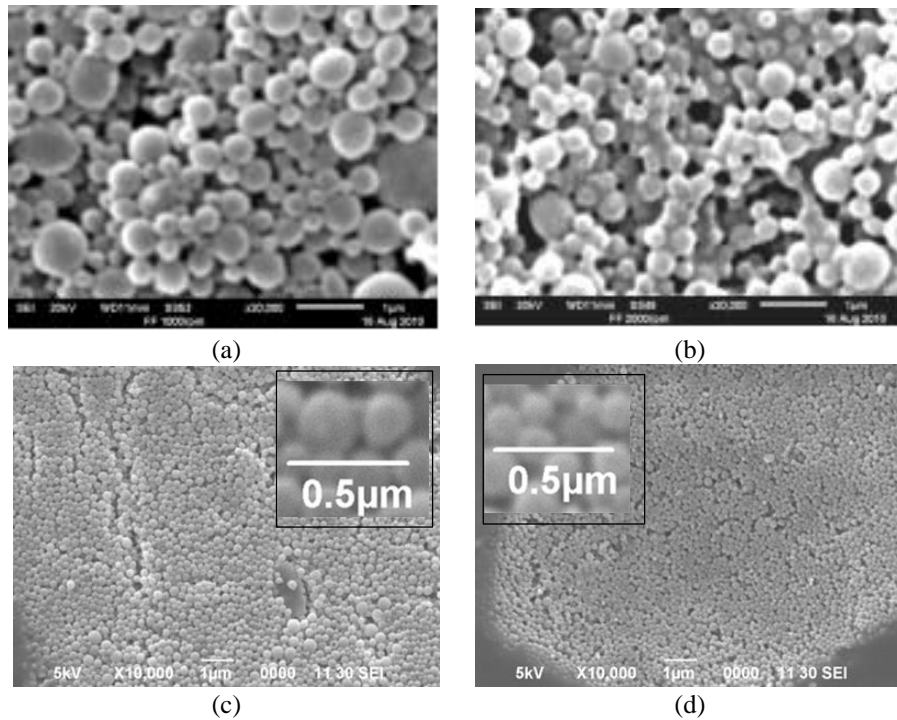


Figure 3. SEM micrograph of MNP-PLA nanosphere samples: (a) S1, (b) S2, (c) S5, and (d) S9

TEM observation results show at Figure 4 still clarify the occurrence of nanosphere agglomeration in S5 and S9 samples in which nanospheres tend to stick to each other at its surface forming nanosphere network instead of bulk agglomeration. This kind of agglomeration is analyzed due to hydrophobic nature of PLA which result in a more preferable bind between carboxylate group of PLA than with OH⁻ group of water medium [5]. These images also show homogeneous dispersion of MNP inside the nanosphere giving end nanosphere size of around 100 nm to 500 nm for S5 sample and around 100 nm to 200 nm for S9 sample. The more clear dispersion of MNPs is shown in Figure 5 of S12 sample. The black spot of around 20 nm of size representing magnetic nanoparticle are observed at the surface of nanosphere surrounded by greyish PLA matrix. These dark spots are in accordance with the size of original MNPs sample. It could be confirmed that MNPs are already separate from each other within PLA matrix forming dilute system instead of core shell system as it found in other magnetic-polymer composite system [13]. Figure 5 also show that after 12,000 centrifugation speed, the supernatant contain single and separate nanosphere of MNP-PLA of around 100 nm.

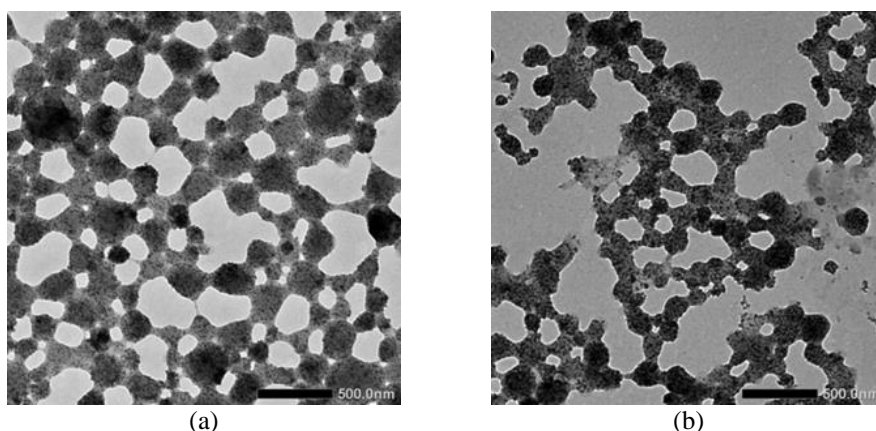


Figure 4. TEM photograph and its particle size distribution curve of (a) sample S5 and (b) sample S9

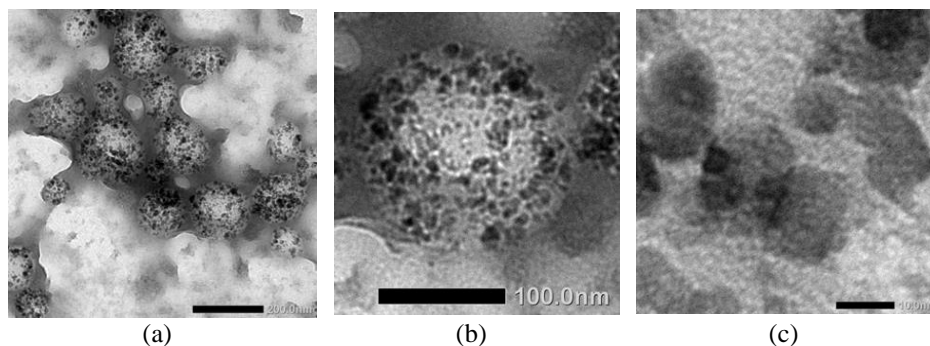


Figure 5. TEM photograph of (a) and (b) S12 sample at different magnification and (c) original MNPs

VSM Measurement

Magnetic materials with the size scale of tens of nanometers typically show superparamagnetic behavior in which the magnetization of nanoparticles will be zero in the absence of external magnetic field, while the coercivity and remanence will be nearly zero in its hysteresis curve [14]. Figure 6 shows hysteresis curve of original oil-based MNPs and its PLA coated nanosphere, which concludes the formation of superparamagnetic behavior of nanoparticle and nanosphere systems. Figure 6(a) shows the M_s value of original MNP is 68.6843 emu/g. The complete M_s values of all precipitate sample are listed in Table 5.

Theoretically, for MNP-PLA nanosphere with the initial composition of 1.2 : 4.2, maximum M_s value of 19.4 emu/g will be obtained. However, the VSM measurements show lower values of M_s for all the samples and give only loading factor in the range of 65% to 78.9%. This decrease was analyzed due to the dilution effect within nanosphere system that causes a weakening of magnetic interaction between the nanoparticles hampered by

the polymer layers. However, surprisingly highest loading factor is achieved for S9 samples which have smaller nanosphere size. Highest M_s value could be related with highest MNP loading and stronger magnetic interaction between the nanosphere, which consequently give heavier nanosphere and easier to precipitate in the centrifugation process. Referring to this data, it could be analyzed that the nanosphere agglomeration due to sticky nature between PLA give more pronounce effect on size distribution behavior than magnetic interaction strength.

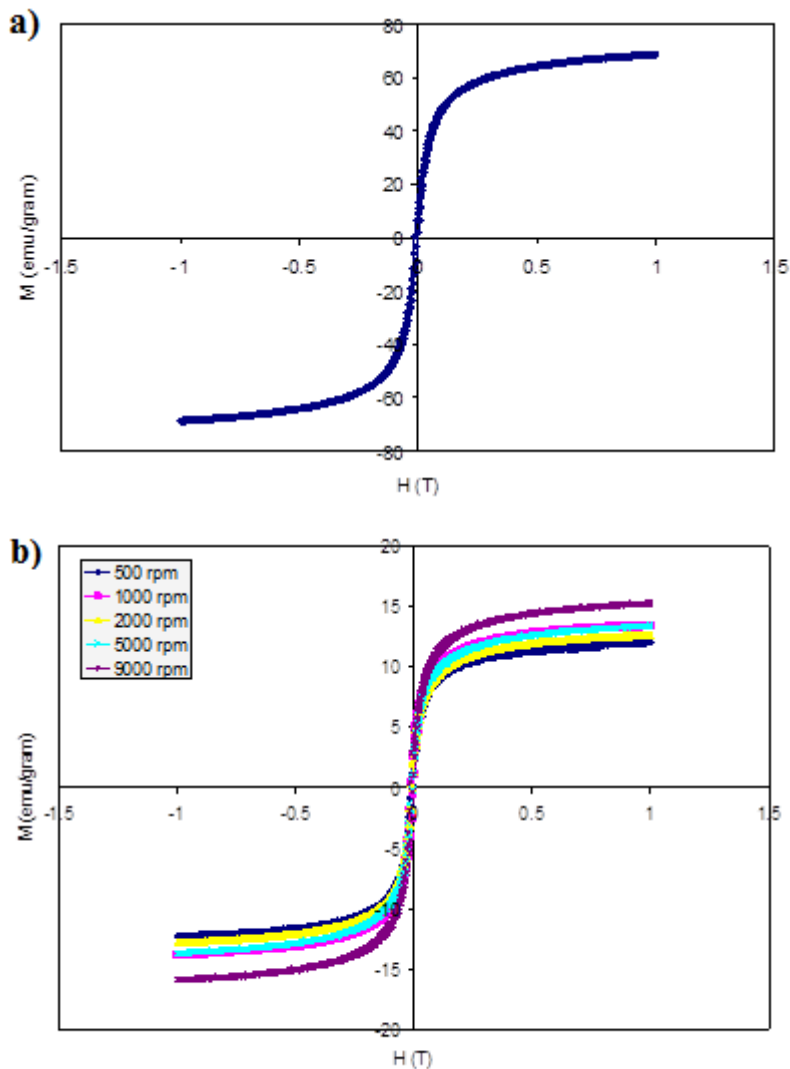


Figure 6. Hysteresis curve of a) original oil-based MNPs and b) its PLA coated nanosphere

Table 4. Ms value of original oil-based MNPs and all precipitate MNPs-PLA samples

No.	Samples	Ms (emu/gram)
1.	Dry MNP	68.6843
2.	P1	13.4978
3.	P2	12.6514
4.	P5	13.4459
5.	P9	15.3041

Discussion

In biomedical applications, for an in-vivo injection process, the formula used is usually in the form of a stable colloid which would enter into the body. Samples will interact with biological units in its path and face a defense mechanism in the body. One of the body's defense mechanisms are macrophages. Macrophage is a type of white blood cell that engulfs and digests foreign substances and anything else that does not have the types of proteins specific to healthy body cells on its surface in a process called phagocytosis [15]. These phagocytes are found in essentially all tissues and take various forms (with various names) throughout the body (e.g., histiocytes, Kupffer cells, alveolar macrophages, microglia and others). Kupffer cells are specialized macrophages located in the liver, lining the walls of the sinusoids that form part of the mononuclear phagocyte system [16].

It is known that, from the structure of the blood vessels, in the vessel wall there are pores as exchange transport media for any substances transferred within the blood to the tissue/fluid surrounding blood vessels. The pore size will vary depending on the type of vessel and the type of tissue that passed, but generally smaller than 15 nm for non-sinusoidal vascular system and ~ 60 nm for sinusoidal vascular system in the form of phagocytosis. While the average diameter of the smallest blood vessels or capillary system is 8 μm [17].

The MNP-PLA nanosphere system would face such body defense mechanism and transportation system, and its accomplishment on reaching any specific target organ will depend on its size and surface properties. The data reported in this research show that nanosphere size will depend on how this parameter is measured. Table 5 presents comparison of particle size measured and observed using different methods.

Table 5. MNP-PLA nanosphere size after sequential size selection and measured with varied methods

Sample	Method	Nanosphere Size (nm)		
		PSA	SEM	TEM
S1		(200 – 3000)	(100 – 1500)	n.a
S2		(250 – 750)	(100 – 900)	n.a
S5		(200 – 500)	(100 – 250)	(100 – 250)
S9		(150 – 450)	(100 – 250)	(100 – 200)
S12		n.a	n.a	(75 – 150)
MNP				< 20 nm

SEM and TEM data indeed already showed that nanosphere are almost homogeneous at nearly 73% mass fraction at the size of around 100 nm as also provided by another research using emulsion and solvent/extraction method [18-19]. This size is only that of dry sample in static nanosphere which represents a single nanosphere size. However, agglomeration tendency could also be acknowledged in the SEM/TEM image. The PSA data on colloidal system gave a more realistic data, because it is measuring the dynamic size of the nanosphere containing the agglomerative nature of the nanosphere. This PSA data of the nanosphere is more reliable when we talk about the transportation within blood circulation system and the size that will be seen by macrophage system. It means, for Fe₃O₄-PLA nanosphere in this report, they could be successfully transported within the blood vessel and nearly all of the injected samples will be captured by phagocytes system especially by Kupffer cells and will be concentrated at liver organ. Some in-vivo tests have proved this argument [9,20]. Intratumoral hyperthermia study of this magnetic-polymer system targeted to epidermoid carcinoma using hEFGR (human epidermal growth factor receptor) showed temperature rise in the tumor region and substantial decrease of tumor volume after 3 w treatment [9]. Other in-vivo biodistribution and hyperthermic study of magnetic-polymer system based on Fe₃O₄-chitosan nanosphere showed also a high heating capacity [13].

To target these sized type of nanoparticles to another organ, which mean avoiding phagocytes trap system, the nanosphere has been modified by PEG to target lung adenocarcinoma A549 cells [21]. However the value of its magnetization was rather low due to due to the introduction of a large amount of PLA-PEG on the surface of MNPs which hindered the capability as a hyperthermia agent.

The heating efficiency of magnetic hyperthermia is usually expressed as Specific Loss Power (SLP) with an equation of [10] :

$$SLP(f, H) = \frac{P(f, H)}{\rho} = \frac{\pi \mu_0 \chi'' H^2 f}{\rho} \quad (1)$$

$$\chi'' = \frac{\omega \tau}{1 + (\omega \tau)^2} \chi_0 \quad (2)$$

$$\chi_0 = \frac{\mu_0 M_s^2 V}{k_B T} \quad (3)$$

H is expressing a given alternating magnetic field with alternating frequency of f , while χ'' denoting imaginary part of the MNP susceptibility, μ_0 is the permeability of free space and ρ is the mass density of the magnetic material. In the second and third equations, τ is the effective magnetic relaxation time, $\omega = 2\pi f$, k_B is the Boltzmann constant, T is the temperature of the sample while V and M_s are the volume and the saturation magnetization of the MNP respectively.

For MNPs to have practical medical applications they should generate large SLP. From these three equations, it could be seen that SLP will depend on χ'' , H , f and ρ . H could only take a low value for lowering damaging effect of high alternating magnetic field to the body. There is also a limited value of frequency of alternating field, f that could be tolerated by the body. Hence, the optimization of SLP is more flexible being carried out by optimizing χ'' and ρ parameters. Equation 2 and 3, state that χ'' parameter is proportional to magnetization, M_s and volume, V of the magnetic nanoparticle. Therefore, higher M_s and bigger size of magnetic nanoparticles will result in higher SLP.

Another factor that could affect SLP that is related to the magnetic nanoparticles is the magnetic anisotropy. The higher the anisotropy of the nanoparticles, the higher the energy would be needed to alternatingly rotate magnetic nanoparticle. Hence, higher SLP will be generated. From equation (1) and (2), it should be emphasized that the SLP is maximized when $\omega \tau = 1$. This means that the frequency of the applied magnetic field must be correlated with the relaxation time with the boundary condition of $\omega \tau = 1$. Increasing the anisotropy results in an increase in the relaxation time and allows the use of lower frequencies of the magnetic field. The most common types of anisotropy are magnetocrystalline anisotropy, surface anisotropy, shape anisotropy, exchange anisotropy; and induced anisotropy (for example, by stress). For nanoparticles, shape anisotropy is the dominant form of anisotropy. Stress anisotropy implies that magnetization might change with stress. It was shown that magnetic anisotropy changes when the surfaces are modified or adsorb different molecules. This means that surface structure significantly influence the magnetic anisotropy. Hence, due to their large

ratio of surface to bulk atoms, the surface anisotropy of nanoparticles could be more significant than both the crystalline and shape anisotropy. Coating of nanoparticles can have an influence on their magnetic anisotropies and hence on their magnetic hyperthermia capabilities.

Referring to the result on this experiment, the size and magnetization of the MNP-PLA nanosphere is potential to be used in hyperthermia especially for targeting cancer treatment on the liver organ. By modifying its surface with PEG to obtain separate nanosphere while maintaining its high magnetization value [18], this MNP-PLA nanosphere could be expected to be targeted to other cancerous cells cite, and give enough heat for killing these cells.

CONCLUSION

The magnetic nanosphere of PLA coated Fe₃O₄ have been synthesized by emulsion method followed by a sequential particle size separation process and characterization to understand the pattern of nanosphere size distribution formation. SEM/TEM observations ensured the formation of homogeneous nanosphere with the size of 100 nm to 200 nm and weight fraction of nearly 73% after separation process with centrifugation at 5000 rpm. However, PSA measurements showed that nanosphere tends to bond to one another and form agglomerations with a size almost double the size of a single nanosphere. Magnetization values only slightly affected by changes in particle size with maximum value reaching 15.3 emu/g, which denotes the maximum loading factor of 78.9%. The combination of the size and the magnetic properties, Fe₃O₄-PLA nanosphere provide a good prospect to be applied in the process of liver cancer therapy with hyperthermia techniques.

ACKNOWLEDGMENT

This work was supported by the DIPA of PSTBM-BATAN at fiscal year of 2015. The authors would like to thank PSTBM-BATAN management for providing this fund. Acknowledgement would also be delivered to Ms. Wildan Zakiah Lbs. for her continuous support during laboratory work and VSM measurement.

REFERENCES

- [1]. Haraldsdóttir KH, Ivarsson K, Götberg S, Ingvar C, Stenram U, Tranberg KG. Interstitial laser thermotherapy (ILT) of breast cancer.

- Eur J Surg Oncol 2008;34(7):739-45.
- [2]. Udroi I. Ultrasonic drug delivery in oncology. JBUON 2015;20(2):381-90.
- [3]. Giustini AJ, Petryk AA, Cassim SM, Tate JA, Baker I, Hoopes PJ. Magnetic nanoparticle hyperthermia in cancer treatment. Nano Life 2013;1:1-23.
- [4]. Wahajuddin, Arora S. Superparamagnetic iron oxide nanoparticles: magnetic nanoplatforms as drug carriers. Int J Nanomedicine 2012;7:3445-71.
- [5]. Hamad K, Kaseem M, Yang HW, Deri F, Ko YG. Properties and medical applications of polylactic acid: A review. eXPRESS Polym Lett 2015;9(5):435-55.
- [6]. Jain DS, Athawale RB, Bajaj AN, Shrikhande SS, Goel PN, Nikam Y, Gude RP. Poly lactic acid (PLA) nanoparticles sustain the cytotoxic action of temozolomide in C6 Glioma cells. Biomed Aging Pathol 2013;3(4):201-8.
- [7]. Ghazanfari MR, Kashefi M, Shams SF, Jaafari MR. Perspective of Fe₃O₄ nanoparticles role in biomedical applications. Biochem Res Int 2016;7840161:1-32.
- [8]. Baldi G, Ravagli C, Mazzantini F, Loudos G, Adan J, Masa M, Psimadas D, Fragogeorgi EA, Locatelli E, Innocenti C, Sangregorio C, Comes Franchini M. In vivo anticancer evaluation of the hyperthermic efficacy of anti-human epidermal growth factor containing magnetic nanoparticles. Int J Nanomedicine 2014;9:3037-56.
- [9]. Shin SW, Song IH, Um SH. Role of physicochemical properties in nanoparticle toxicity. Nanomaterials 2015;5:1351-65.
- [10]. Obaidat IM, Issa B, Haik Y. Magnetic properties of magnetic nanoparticles for efficient hyperthermia. Nanomaterials 2015;5:63-89.
- [11]. Leamy PJ. Preparation, characterization, and in-vitro testing of poly(lactide-co-glycolide) and dextran magnetic microspheres for in-vivo applications. Thesis PhD University of Florida, 2003:AAI3128852.
- [12]. Hapsari BW, Mujamilah, Kurniati M, Sulungbudi GT. Sintesis nanosfer berbasis ferrofluid dan poly lactic acid dengan metoda sonikasi. J Sains Mater Indonesia 2007;11(2):139-44.
- [13]. Patil RM, Shete PB, Thorat ND, Otari SV, Barick KC, Prasad A, Ningthoujam RS, Tiwale BM, Pawar SH. Superparamagnetic iron oxide/chitosan core/shells for hyperthermia application: Improved colloidal stability and biocompatibility. J Magn Magn Mater 2014;355:22-30.
- [14]. Bean CP, Livingston JD. Superparamagnetism. J Appl Phys 1959;30(4):S120-9.

- [15]. Aderem A, Underhill DM. Mechanism of Phagocytosis in Macrophages. *Annu Rev Immunol* 1999;17:593-623.
- [16]. Dixon LJ, Barnes M, Tang H, Pritchard MT, Laura E, Clinch C. Kupffer Cells in the Liver. *Compr Physiol* 2013;3(2):785-97.
- [17]. Sarin H. Physiologic upper limits of pore size of different blood capillary types and another perspective on the dual pore theory of microvascular permeability. *J Angiogenesis Res* 2010;2(14):1-19.
- [18]. Yang G, Zhang B, Wang J, Wang M, Xie S, Li X. Synthesis and characterization of poly (lactic acid)-modified superparamagnetic iron oxide nanoparticles. *J Sol-Gel Sci Technol* 2015;77:335-41.
- [19]. Hu FX, Neoh KGA, Kang ET. Synthesis and in vitro anti-cancer evaluation of tamoxifen-loaded magnetite/PLLA composite nanoparticles. *Biomaterials* 2006;27:5725-33.
- [20]. Lee PW, Hsu SH, Wang JJ, Tsai JS, Lin KJ, Wey SP, Chen FR, Lai CH, Yen TC, Sung HW. The characteristics, biodistribution, magnetic resonance imaging, and biodegradability of superparamagnetic core – shell nanoparticles. *Biomaterials* 2010;31:1316-24.
- [21]. Kim HC, Kim E, Jeong SW, Ha T-L, Park S-I, Lee SG, Lee SW. Nanoscale micelles for combined hyperthermia and chemotherapy. *Nanoscale* 2015;7:16470-80.